Journal of Thermal Analysis, Vol. 48 (1997) 981-988

EFFECT OF BaF_2 IN THE FORMATION OF Y_2BaCuO_5 PARTICLES IN Y–Ba–Cu–O SUPERCONDUCTOR

Tsugio Hamada, Kei-ichi Iida and Kenji Mitsuda

Department of Electrical Engineering, Miyakonozyo College of Technology, 473–1 Yoshio, Miyakonozyo 885, Japan

Abstract

The YBCO superconductor was synthesized with BaF_2. The synthesis temperature of the specimen with BaF_2 was to be considerably lower than that for the unused one. The BaF_2 decomposes during the heat treatment, and does not influence the structure and critical temperature. The critical current density, J_c, in the specimen is 1×10^8 A/m^2 at 77 K and 0.5 *T*. However, J_c is actually lower for the QMG specimen because the Y_2BaCuO_5 particles are larger than those of the QMG specimen.

Keywords: BaF_2, critical current density, synthesis temperature, Y_2BaCuO_5 particle

Introduction

The critical current density, J_c, is determined by the pinning strength of the pinning center in the superconducting matrix. Y_2BaCuO_5 is well known to act as a pinning center in YBCO [1–3]. The Y_2BaCuO_5 particles in the superconducting matrix generally originate at temperatures above 1000°C. Typical methods to distribute the Y_2BaCuO_5 particles finely in the matrix are quench and melt growth (QMG) [2], melt textured growth and powder melt growth. The materials prepared by means of these methods have larger critical current densities than those prepared by conventional methods. However, it is not easy to apply such materials to tape wires because they need to be heat-treated at temperatures above 1000°C [4]. In the process of manufacturing the materials into tape wire, it is necessary to cover the surface of the superconducting tape wires with silver sheath to protect the material from oxygen release. However, the melting point of silver is less than 1000°C. Therefore, it is important to decrease the synthesis temperature of the high-temperature superconductors to apply them to tape wires. We use BaF_2 in the synthesis process for this purpose. YBCO superconductor is synthesized at a lower synthesis temperature than usual. In other fields, fluorine has been used to increase the critical temperature due to the interchange of fluorine for oxygen. However, it is not easy to exchange oxygen with fluorine in the synthesis process. We have observed that BaF_2 influences the interchange of the Y_2BaCuO_5 particles in the matrix without influencing the critical temperature. In this paper, YBCO specimens are investigated as concerns the behavior of BaF_2 in superconductors. The techniques applied were differential thermal analysis (DTA), scanning electron microscopy (SEM), X-ray diffractometry (XRD) and electron probe microanalysis (EPMA).

0368–4466/97/ $ 5.00

John Wiley & Sons Limited
Chichester

Experimental

Specimen

The specimens used in this study were prepared from $YBa_2Cu_3O_x$ and $YBa_2Cu_3F_4O_x$ powders. $YBa_2Cu_3O_x$ powder was synthesized from Y_2O_3, $BaCO_3$ and CuO. $YBa_2Cu_3F_4O_x$ powder was synthesized from Y_2O_3, BaF_2 and CuO [5]. The two master compositions, $YBa_2Cu_3O_x$ and $YBa_2Cu_3F_4O_x$, were calcined at 900°C for 8 h in air. They were then cooled to room temperature and were ground again in a mortar. They were mixed to yield $YBa_2Cu_3F_{0.4}O_x$ specimen (#1), which was sintered at 950°C for 2 h and was then cooled to room temperature at a cooling rate of 2°C h^{-1}. Specimen #1 exhibited a large hysteresis loop, as in metallic superconductors, with strong pinning strength [6]. Thus, the molar ratio 0.4 mol fluorine was selected. $YBa_2Cu_3O_x$ (#2) was used for comparison with specimen #1.

Measurements

Specimens #1 and #2 were subjected to DTA and TG at temperatures up to 1100°C. The observations of microstructures were carried out for specimens with their surfaces polished like mirrors. The Y_2BaCuO_5 particles were observed by SEM and XRD in specimens #1 and #2. Composition analysis was carried out by EPMA. Magnetic properties were measured with a SQUID magnetometer [7].

Results and discussion

DTA and TG

DTA and TG were performed on specimens #1 and #2 at temperatures up to 1100°C in air. The experimental conditions were as follows: sampling rate 1.0 s, increasing temperature rate 10°C min^{-1} and a platinum thermocouple. The results are shown in Figs 1(a) and 1(b), respectively. In the DTA curve, four endothermal peaks are to be seen above 800°C (Fig. 1(a)).

Endothermal peaks are generally interpreted as transitions of melting and/or crystallization. The largest peak was observed at 938°C for specimen #1 [8], but at above 1000°C for specimen #2 (Fig. 1(b)). If we assume that the large peaks reflect the transition of melting in the powder specimens, it seems that powder specimen #1 partly melts at the temperature of the peak. If so, the melting temperature was decreased by about 100°C in comparison with specimen #2. However, the two powder specimens did not completely melt at these temperatures, for the powder specimens practically preserved their form. The TG curves revealed mass losses for both specimens above 800°C. Sharp variations are to be seen in the vicinity of the largest endothermal peaks for the two specimens in Figs 1(a) and 1(b). They seemed to lose part of the specimen into the air. Thus, it is necessary to investigate the behavior of BaF_2 on the synthesis of the superconductor during the heat treatment. Firstly, quenched specimens were used to clarify the behavior of BaF_2. X-ray diffraction patterns were measured for specimens quenched from 900 and 950°C [8], the largest DTA peak in Fig. 1(a) existing between 900 and 950°C.

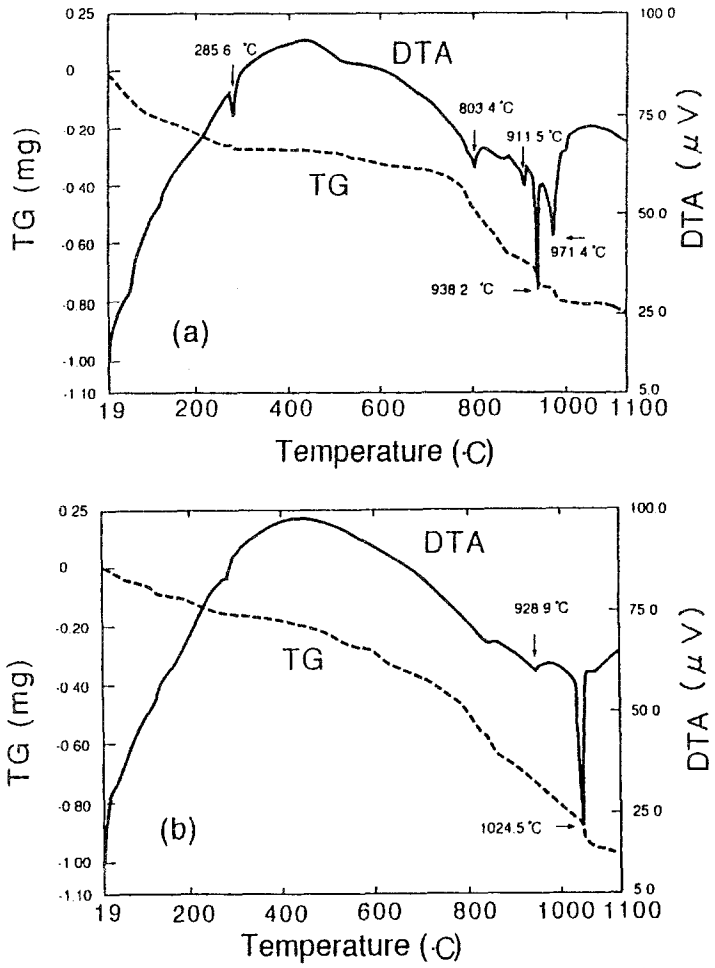

Fig. 1 DTA and TG for specimens #1 and #2. For specimen #1 (a) large endothermic peaks were observed at temperatures above 800°C. The largest peak was situated about 100°C lower than that for specimen #2 (b)

The results are shown in Fig. 2. Some peaks in the pattern of the quenched specimen agreed with the BaF_2 peaks. Hence, the BaF_2 in the starting material did not react completely during the heat treatment. However, BaF_2 was also present in the specimen quenched from 950°C. It was also necessary to investigate in detail the relationship between BaF_2 and the largest DTA peak at 938°C. For this, specimens quenched from several temperatures were prepared and investigated.

EPMA and XRD analysis

The existence of BaF_2 in the specimen was investigated by using specimens quenched from 700, 800, 900, 935 and 950°C [9]. Here, the temperatures of 800

and 900°C include two data, for increase and decrease of the temperature from the maximum temperature. In this case the data of decreasing temperature 700 and 900°C are excluded from the data (Fig. 2). The BaF_2 peaks decreased as the quenching temperature was increased. The F concentration was analysed on an area of 25×25 μm on the polished surface of each specimen. The results are shown in Fig. 3. With increase of the quenching temperature, the percentage of F on the surface increased. This indicates that BaF_2 in the specimen was decomposed into its unit components at temperatures from 900 to 950°C. Additionally, the F moved towards the surface of the specimen so that the surface percentage of F increased. However, the specimen quenched from 950°C gave BaF_2 peaks in the XRD pattern. This seems to be due to the heterogeneity of the specimen. Microstructural observations of the polished surfaces of the specimens were carried out for the specimens quenched from 700, 800, 900 and 935°C. The above specimens 935 and 800°C are quenched at the given temperature in a cooling process *via* the maximum temperature 950°C. The results are shown in Fig. 4. At 700°C, the specimen was in a condition of granularity. However, the grains seem to melt on increase of temperature. This agrees with the DTA finding, where the peaks appeared at temperatures above 900°C, i.e. in specimen #1 partial melting occurred at a lower temperature than that for specimen #2. The melted part of the specimen increased at temperatures up to 950°C. The Y_2BaCuO_5 phase became visible as particles (Fig. 4). In the same proc-

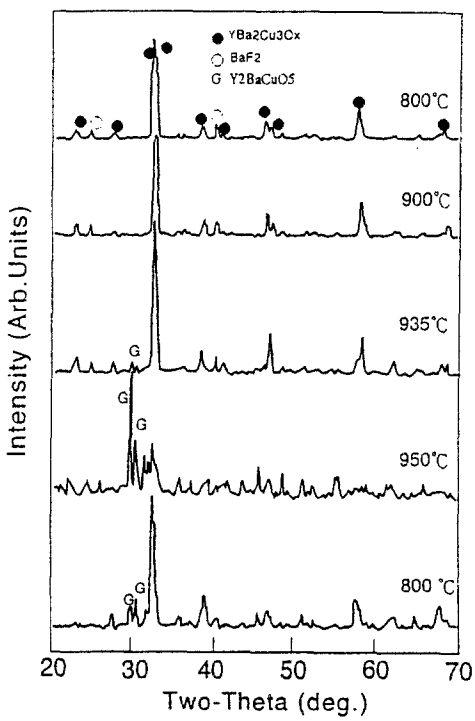

Fig. 2 XRD patterns for the quenched specimens. The superconducting phases exist at 800°C, while the BaF_2 phase exists simultaneously in the patterns up to 950°C. The pattern at 800°C in the process of decrease of temperature does not contain BaF_2 peaks

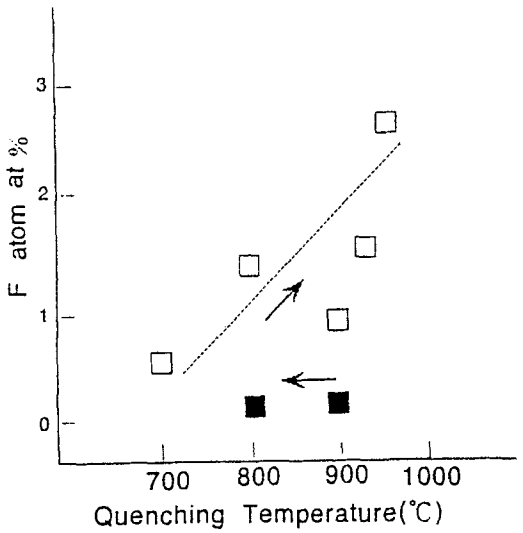

Fig. 3 Concentration of F *vs.* quenching temperature for quenched specimens. The percentage F increases as the temperature is increased (□); in the process of temperature decrease from 800 and 900°C, the specimens hardly contain F (■)

ess, no Y_2BaCuO_5 particles were seen in the matrix of specimen #2. Quantitative analysis of the particles was done elsewhere [9]. On the other hand, the $YBa_2Cu_3O_x$ and Y_2BaCuO_5 phases were observed in the XRD pattern. The Y_2BaCuO_5 phase did not appear in the XRD pattern for the unused sample [10]. It seems that BaF_2 influences formation of the Y_2BaCuO_5 phase. We examined the influence of BaF_2 on the structure of $YBa_2Cu_3O_x$. The lattice parameters were calculated from the Bragg equation for the superconducting peaks, and we obtained average values of $a=3.90$ Å, $b=3.85$ Å and $c=11.70$ Å for the specimens (Fig. 5). In another report [11], the early quenched specimens had the parameters of tetragonal $YBa_2Cu_3O_x$. However, the obtained values did not display any tendency to a temperature dependence: the lattice parameters were virtually constant for different quenching temperatures. The decomposition and evaporation of BaF_2 did not influence the structure [12].

Critical current density

The critical current density was estimated from DC magnetization measurements. The results of critical current density *vs.* magnetic field are shown in Fig. 6 for specimen #1. J_c was 1×10^8 A m^{-2} at 77 K and 0.5 *T*. At a lower temperature and the same applied field, the critical current density increased to 10^9 A m^{-2}. However, these J_c values are actually inferior to that for the QMG specimen, possibly because the non-superconducting Y_2BaCuO_5 particles in the QMG specimen are finely distributed in the matrix (less than 1 μm), whereas in specimen #1 they are distributed as large particles (Fig. 4). In the microstructure, the Y_2BaCuO_5 particles are practically distributed throughout the matrix. This reflects the fluxoid mo-

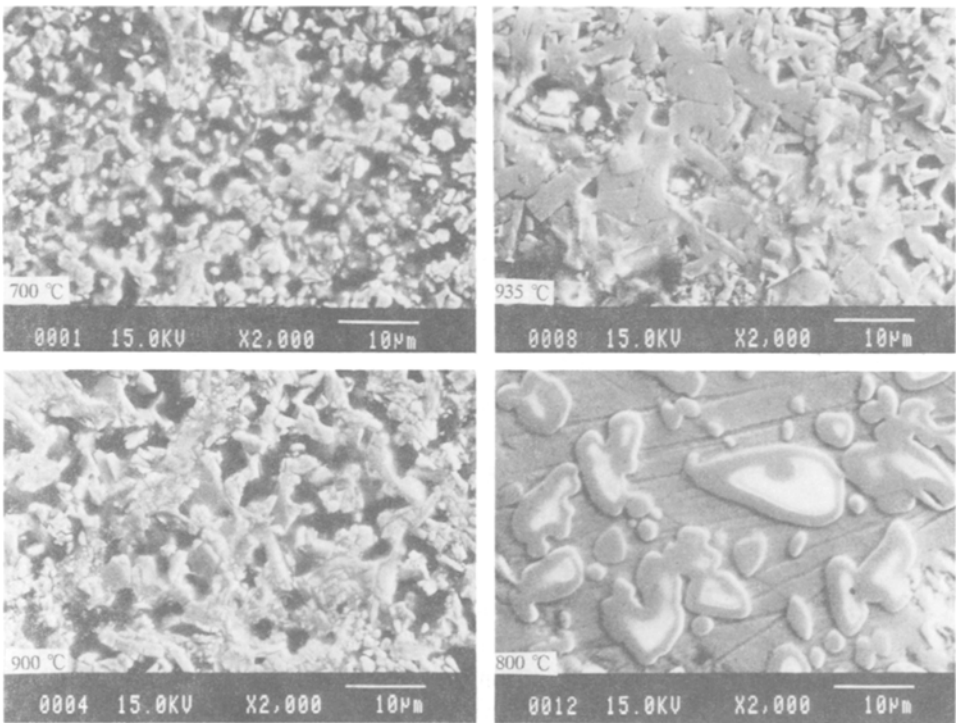

Fig. 4 Microstructural observations for quenched specimens at several temperatures. At the early quenched temperature, the microstructure was granular, but the Y_2BaCuO_5 phase appeared as particles in the matrix in the specimen quenched from 800°C

tion against the Lorentz force. J_c in superconductors is determined by the pinning strength; it is related to the Lorentz and pinning forces by the expression $F_p=J_cB$. Our experimental results indicate that the typical size of the Y_2BaCuO_5 particles is of the order of 5 μm and usually much larger than the fluxoid spacing a_f. We assume that the fluxoid size is 2ζ in diameter and has no anisotropy. In the superconducting state, the energy is lower and more stable than in the normal state. The energy difference is expressed as $B_c^2/2\mu_o$ per unit volume, where B_c is the thermodynamic critical field. If the Y_2BaCuO_5 particle has a diameter D, the loss of condensation energy is less than $(B_c^2/2\mu_o)\pi\zeta^2 D$ for each fluxoid when it meets the normal particle [13]. Thus, the elementary pinning force for the normal particles is approximately given by

$$F_P = \frac{\pi\tau\zeta B_C^2}{4Da_f\mu_o}\left(1-\frac{B}{B_{c2}}\right)^2$$

where μ_o is the permeability in vacuum, a_f is the fluxoid spacing, calculated as $a_f=(2\Phi_o/\sqrt{3}B)^{1/2}$, B_c is the thermodynamic critical field, τ is the volume fraction of the normal particles in the specimen, and ζ is the coherence length. It is found from

the above equation that the elemental pinning force becomes larger as D decreases and τ increases. Therefore, to increase the critical current density, it is necessary for Y_2BaCuO_5 particles to distribute more finely in the matrix with high density.

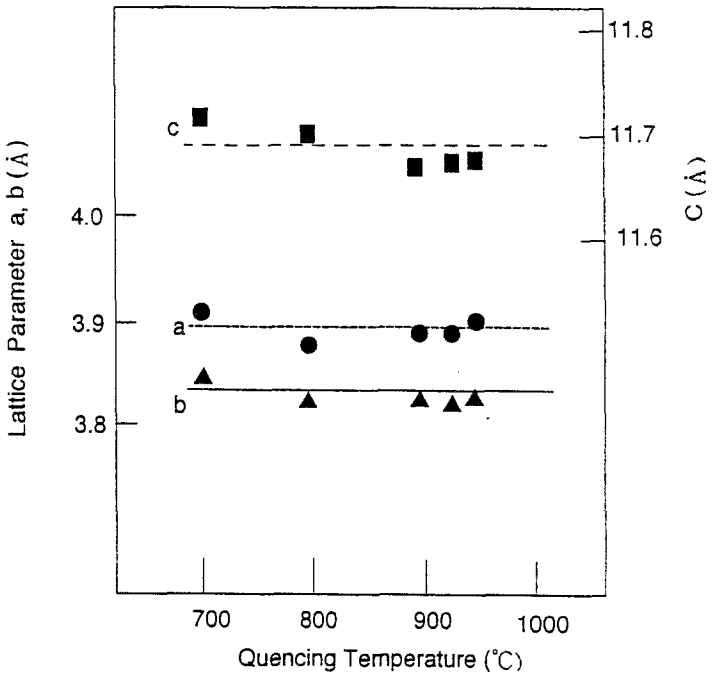

Fig. 5 Lattice parameters parameters a, b and c *vs.* quenching temperature. Average values of $a=3.90$ Å, $b=3.85$ Å and $c=11.70$ Å were found. These parameters hardly changed with variation of the quenching temperature

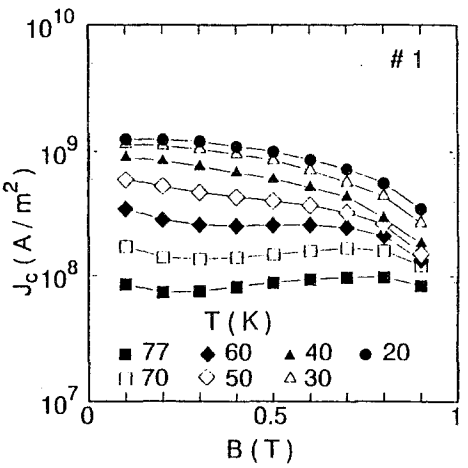

Fig. 6 Critical current density *vs.* magnetic field for specimen #1. J_c was 1×10^8 A m^{-2} at 77 K and 0.5 T

The synthesis temperature was much lower than in the QMG process. Hence, a silver sheath tube covered on the surface will be able to endure the heat in the high-temperature treatment. However, we have not yet examined this for YBCO materials. For more progress, it is necessary to convert bulk material to tape wires.

Conclusions

An YBCO superconductor with BaF_2 was synthesized at a lower synthesis temperature than usual. The behavior of the BaF_2 was investigated as concerns the superconductor and the critical current densities. The results obtained were as follows:

(1) The temperature of synthesis of the specimen with BaF_2 was about 100°C lower than that for the unused specimen.

(2) The crystal structures hardly changed with variation of the quenching temperature. The decomposition and evaporation of BaF_2 did not influence the structure.

(3) The obtained J_c was lower for the QMG specimen; to increase the critical current density, it is necessary for Y_2BaCuO_5 particles to distribute more finely in the matrix with high density.

* * *

We authors would like to thank Drs M. Kashiwabara and T. Minamitake for their help with the experiments. We are also indebted to Y. Hamada, Y. Ueno and Y. Nakamura for preparation of the manuscript.

References

1 T. Matsushita, B. Ni and K. Yamafuji, Adv. Cryogenic Engin., 36 (1990) 403.
2 H. Fujimoto, M. Murakami and N. Koshizuka, Physica C, 203 (1992) 103.
3 M. Murakami, H. Fujimoto, S. Gotoh, K. Yamaguchi, N. Koshizuka and S. Tanaka, Physica C, 185 (1991).
4 M. Murakami, M. Morita, K. Miyamoto and S. Matsuda, Prog. in High Temperature Superconductivity, World Scientific, Singapore 1989, p. 95.
5 S. R. Ovshinsky, R. T. Young, D. D. Allred, G. DeMaggio and G. A. Van der Leeden, Phys. Rev. Lett., 58 (1987) 2579.
6 F. Sumiyoshi, T Hamada and S. Kawabata, Cryogenics, 28 (1988) 3.
7 Nozomu Ohtani, Edmund Soji Otabe, Teruo Matsushita and Baorong Ni, Jpn. J. Appl. Phys., 31 (1992) L169.
8 T. Hamada and R. Morimo, Phys. Stat. Sol. (a), 145 (1994) 61.
9 T. Hamada, R. Morimo and R. Ogura, J. Mater. Sci., 31 (1996) 2579.
10 T. Hamada and R. Morimo, Phys. Stat. Sol. (a), 151 (1995) 199.
11 Seiji Adachi, Takeohi Sakurai, Yuji Yaegashi, Nobuaki Seiji, Atsushi Fukuoka and H. Yamauchi, Phisica C, 206 (1993) 329.
12 T. Hamada and T. Nomachi, Phys. Stat. Sol. (a), 153 (1996) 165.
13 T. Hamada, Y. Ohzono, T. Akune and N. Sakamoto, J. Mater. Sci., 32 (1997) 1021.